

Measurement of J/ψ and $\psi(2S)$ Polarization in $p\bar{p}$ Collisions at $\sqrt{s} = 1.8$ TeV

T. Affolder,²¹ H. Akimoto,⁴³ A. Akopian,³⁶ M. G. Albrow,¹⁰ P. Amaral,⁷ S. R. Amendolia,³² D. Amidei,²⁴ K. Anikeev,²² J. Antos,¹ G. Apollinari,¹⁰ T. Arisawa,⁴³ T. Asakawa,⁴¹ W. Ashmanskas,⁷ M. Atac,¹⁰ F. Azfar,²⁹ P. Azzi-Bacchetta,³⁰ N. Bacchetta,³⁰ M. W. Bailey,²⁶ S. Bailey,¹⁴ P. de Barbaro,³⁵ A. Barbaro-Galtieri,²¹ V. E. Barnes,³⁴ B. A. Barnett,¹⁷ M. Barone,¹² G. Bauer,²² F. Bedeschi,³² S. Belforte,⁴⁰ G. Bellettini,³² J. Bellinger,⁴⁴ D. Benjamin,⁹ J. Bensinger,⁴ A. Beretvas,¹⁰ J. P. Berge,¹⁰ J. Berryhill,⁷ B. Bevensee,³¹ A. Bhatti,³⁶ M. Binkley,¹⁰ D. Bisello,³⁰ R. E. Blair,² C. Blocker,⁴ K. Bloom,²⁴ B. Blumenfeld,¹⁷ S. R. Blusk,³⁵ A. Bocci,³² A. Bodek,³⁵ W. Bokhari,³¹ G. Bolla,³⁴ Y. Bonushkin,⁵ D. Bortoletto,³⁴ J. Boudreau,³³ A. Brandl,²⁶ S. van den Brink,¹⁷ C. Bromberg,²⁵ M. Brozovic,⁹ N. Bruner,²⁶ E. Buckley-Geer,¹⁰ J. Budagov,⁸ H. S. Budd,³⁵ K. Burkett,¹⁴ G. Busetto,³⁰ A. Byon-Wagner,¹⁰ K. L. Byrum,² P. Calafiura,²¹ M. Campbell,²⁴ W. Carithers,²¹ J. Carlson,²⁴ D. Carlsmith,⁴⁴ J. Cassada,³⁵ A. Castro,³⁰ D. Cauz,⁴⁰ A. Cerri,³² A. W. Chan,¹ P. S. Chang,¹ P. T. Chang,¹ J. Chapman,²⁴ C. Chen,³¹ Y. C. Chen,¹ M.-T. Cheng,¹ M. Chertok,³⁸ G. Chiarelli,³² I. Chirikov-Zorin,⁸ G. Chlachidze,⁸ F. Chlebana,¹⁰ L. Christofek,¹⁶ M. L. Chu,¹ C. I. Ciobanu,²⁷ A. G. Clark,¹³ A. Connolly,²¹ J. Conway,³⁷ J. Cooper,¹⁰ M. Cordelli,¹² J. Cranshaw,³⁹ D. Cronin-Hennessy,⁹ R. Cropp,²³ R. Culbertson,⁷ D. Dagenhart,⁴² F. DeJongh,¹⁰ S. Dell'Agnello,¹² M. Dell'Orso,³² R. Demina,¹⁰ L. Demortier,³⁶ M. Deninno,³ P. F. Derwent,¹⁰ T. Devlin,³⁷ J. R. Dittmann,¹⁰ S. Donati,³² J. Done,³⁸ T. Dorigo,¹⁴ N. Eddy,¹⁶ K. Einsweiler,²¹ J. E. Elias,¹⁰ E. Engels, Jr.,³³ W. Erdmann,¹⁰ D. Errede,¹⁶ S. Errede,¹⁶ Q. Fan,³⁵ R. G. Feild,⁴⁵ C. Ferretti,³² R. D. Field,¹¹ I. Fiori,³ B. Flaugher,¹⁰ G. W. Foster,¹⁰ M. Franklin,¹⁴ J. Freeman,¹⁰ J. Friedman,²² Y. Fukui,²⁰ I. Furic,²² S. Galeotti,³² M. Gallinaro,³⁶ T. Gao,³¹ M. Garcia-Sciveres,²¹ A. F. Garfinkel,³⁴ P. Gatti,³⁰ C. Gay,⁴⁵ S. Geer,¹⁰ D. W. Gerdes,²⁴ P. Giannetti,³² P. Giromini,¹² V. Glagolev,⁸ M. Gold,²⁶ J. Goldstein,¹⁰ A. Gordon,¹⁴ A. T. Goshaw,⁹ Y. Gotra,³³ K. Goulianos,³⁶ C. Green,³⁴ L. Groer,³⁷ C. Grosso-Pilcher,⁷ M. Guenther,³⁴ G. Guillian,²⁴ J. Guimaraes da Costa,¹⁴ R. S. Guo,¹ R. M. Haas,¹¹ C. Haber,²¹ E. Hafen,²² S. R. Hahn,¹⁰ C. Hall,¹⁴ T. Handa,¹⁵ R. Handler,⁴⁴ W. Hao,³⁹ F. Happacher,¹² K. Hara,⁴¹ A. D. Hardman,³⁴ R. M. Harris,¹⁰ F. Hartmann,¹⁸ K. Hatakeyama,³⁶ J. Hauser,⁵ J. Heinrich,³¹ A. Heiss,¹⁸ M. Herndon,¹⁷ B. Hinrichsen,²³ K. D. Hoffman,³⁴ C. Holck,³¹ R. Hollebeek,³¹ L. Holloway,¹⁶ R. Hughes,²⁷ J. Huston,²⁵ J. Huth,¹⁴ H. Ikeda,⁴¹ J. Incandela,¹⁰ G. Introzzi,³² J. Iwai,⁴³ Y. Iwata,¹⁵ E. James,²⁴ H. Jensen,¹⁰ M. Jones,³¹ U. Joshi,¹⁰ H. Kambara,¹³ T. Kamon,³⁸ T. Kaneko,⁴¹ K. Karr,⁴² H. Kasha,⁴⁵ Y. Kato,²⁸ T. A. Keaffaber,³⁴ K. Kelley,²² M. Kelly,²⁴ R. D. Kennedy,¹⁰ R. Kephart,¹⁰ D. Khazins,⁹ T. Kikuchi,⁴¹ B. Kilminster,³⁵ M. Kirby,⁹ M. Kirk,⁹ B. J. Kim,¹⁹ D. H. Kim,¹⁹ H. S. Kim,¹⁶ M. J. Kim,¹⁹ S. H. Kim,⁴¹ Y. K. Kim,²¹ L. Kirsch,⁴ S. Klimentenko,¹¹ P. Koehn,²⁷ A. Königeter,¹⁸ K. Kondo,⁴³ J. Konigsberg,¹¹ K. Kordas,²³ A. Korn,²² A. Korytov,¹¹ E. Kovacs,² J. Kroll,³¹ M. Kruse,³⁵ S. E. Kuhlmann,² K. Kurino,⁴⁵ T. Kuwabara,⁴¹ A. T. Laasanen,³⁴ N. Lai,⁷ S. Lami,³⁶ S. Lammel,¹⁰ J. I. Lamoureux,⁴ M. Lancaster,²¹ G. Latino,³² T. LeCompte,² A. M. Lee IV,⁹ K. Lee,³⁹ S. Leone,³² J. D. Lewis,¹⁰ M. Lindgren,⁵ T. M. Liss,¹⁶ J. B. Liu,³⁵ Y. C. Liu,¹ N. Lockyer,³¹ J. Loken,²⁹ M. Loretto,³⁰ D. Lucchesi,³⁰ P. Lukens,¹⁰ S. Lusin,⁴⁴ L. Lyons,²⁹ J. Lys,²¹ R. Madrak,¹⁴ K. Maeshima,¹⁰ P. Maksimovic,¹⁴ L. Malferrari,³ M. Mangano,³² M. Mariotti,³⁰ G. Martignon,³⁰ A. Martin,⁴⁵ J. A. J. Matthews,²⁶ J. Mayer,²³ P. Mazzanti,³ K. S. McFarland,³⁵ P. McIntyre,³⁸ E. McKigney,³¹ M. Menguzzato,³⁰ A. Menzione,³² C. Mesropian,³⁶ T. Miao,¹⁰ R. Miller,²⁵ J. S. Miller,²⁴ H. Minato,⁴¹ S. Miscetti,¹² M. Mishina,²⁰ G. Mitselmakher,¹¹ N. Moggi,³ E. Moore,²⁶ R. Moore,²⁴ Y. Morita,²⁰ M. Mulhearn,²² A. Mukherjee,¹⁰ T. Muller,¹⁸ A. Munar,³² P. Murat,¹⁰ S. Murgia,²⁵ M. Musy,⁴⁰ J. Nachtman,⁵ S. Nahn,⁴⁵ H. Nakada,⁴¹ T. Nakaya,⁷ I. Nakano,¹⁵ C. Nelson,¹⁰ D. Neuberger,¹⁸ C. Newman-Holmes,¹⁰ C.-Y. P. Ngan,²² P. Nicolaidi,⁴⁰ H. Niu,⁴ L. Nodulman,² A. Nomerotski,¹¹ S. H. Oh,⁹ T. Ohmoto,¹⁵ T. Ohsugi,¹⁵ R. Oishi,⁴¹ T. Okusawa,²⁸ J. Olsen,⁴⁴ W. Orejudos,²¹ C. Pagliarone,³² F. Palmonari,³² R. Paoletti,³² V. Papadimitriou,³⁹ S. P. Pappas,⁴⁵ D. Partos,⁴ J. Patrick,¹⁰ G. Pauletta,⁴⁰ M. Paulini,²¹ C. Paus,²² L. Pescara,³⁰ T. J. Phillips,⁹ G. Piacentino,³² K. T. Pitts,¹⁶ R. Plunkett,¹⁰ A. Pompos,³⁴ L. Pondrom,⁴⁴ G. Pope,³³ M. Popovic,²³ F. Prokoshin,⁸ J. Proudfoot,² F. Ptohos,¹² O. Pukhov,⁸ G. Punzi,³² K. Ragan,²³ A. Rakitine,²² D. Reher,²¹ A. Reichold,²⁹ W. Riegler,¹⁴ A. Ribon,³⁰ F. Rimondi,³ L. Ristori,³² W. J. Robertson,⁹ A. Robinson,²³ T. Rodrigo,⁶ S. Rolli,⁴² L. Rosenson,²² R. Roser,¹⁰ R. Rossin,³⁰ A. Safonov,³⁶ W. K. Sakumoto,³⁵ D. Saltzberg,⁵ A. Sansoni,¹² L. Santi,⁴⁰ H. Sato,⁴¹ P. Savard,²³ P. Schlabach,¹⁰ E. E. Schmidt,¹⁰ M. P. Schmidt,⁴⁵ M. Schmitt,¹⁴ L. Scodellaro,³⁰ A. Scott,⁵ A. Scribano,³² S. Segler,¹⁰ S. Seidel,²⁶ Y. Seiya,⁴¹ A. Semenov,⁸ F. Semeria,³ T. Shah,²² M. D. Shapiro,²¹ P. F. Shepard,³³ T. Shibayama,⁴¹ M. Shimojima,⁴¹ M. Shochet,⁷ J. Siegrist,²¹ G. Signorelli,³² A. Sill,³⁹ P. Sinervo,²³ P. Singh,¹⁶ A. J. Slaughter,⁴⁵ K. Sliwa,⁴² C. Smith,¹⁷ F. D. Snider,¹⁰ A. Solodsky,³⁶ J. Spalding,¹⁰ T. Speer,¹³ P. Sphicas,²² F. Spinella,³² M. Spiropulu,¹⁴ L. Spiegel,¹⁰ J. Steele,⁴⁴ A. Stefanini,³² J. Strologas,¹⁶ F. Strumia,¹³ D. Stuart,¹⁰ K. Sumorok,²² T. Suzuki,⁴¹ T. Takano,²⁸ R. Takashima,¹⁵ K. Takikawa,⁴¹ P. Tamburello,⁹

M. Tanaka,⁴¹ B. Tannenbaum,⁵ W. Taylor,²³ M. Tecchio,²⁴ P. K. Teng,¹ K. Terashi,⁴¹ S. Tether,²² D. Theriot,¹⁰
 R. Thurman-Keup,² P. Tipton,³⁵ S. Tkaczyk,¹⁰ K. Tollefson,³⁵ A. Tollestrup,⁴⁰ H. Toyoda,²⁸ W. Trischuk,²³
 J. F. de Troconiz,¹⁴ J. Tseng,²² N. Turini,³² F. Ukegawa,⁴¹ T. Vaiciulis,³⁵ J. Valls,³⁷ S. Vejcek III,¹⁰ G. Velev,¹⁰
 R. Vidal,¹⁰ R. Vilar,⁶ I. Volobouev,²¹ D. Vucinic,²² R. G. Wagner,² R. L. Wagner,¹⁰ J. Wahl,⁷ N. B. Wallace,³⁷
 A. M. Walsh,³⁷ C. Wang,⁹ C. H. Wang,¹ M. J. Wang,¹ T. Watanabe,⁴¹ D. Waters,²⁹ T. Watts,³⁷ R. Webb,³⁸ H. Wenzel,¹⁸
 W. C. Wester III,¹⁰ A. B. Wicklund,² E. Wicklund,¹⁰ H. H. Williams,³¹ P. Wilson,¹⁰ B. L. Winer,²⁷ D. Winn,²⁴
 S. Wolbers,¹⁰ D. Wolinski,²⁴ J. Wolinski,²⁵ S. Wolinski,²⁴ S. Worm,²⁶ X. Wu,⁴³ J. Wyss,³² A. Yagil,¹⁰
 W. Yao,²¹ G. P. Yeh,¹⁰ P. Yeh,¹ J. Yoh,¹⁰ C. Yosef,²⁵ T. Yoshida,²⁸ I. Yu,¹⁹ S. Yu,³¹ Z. Yu,⁴⁵ A. Zanetti,⁴⁰
 F. Zetti,²¹ and S. Zucchelli³

(CDF Collaboration)

¹*Institute of Physics, Academia Sinica, Taipei, Taiwan 11529, Republic of China*

²*Argonne National Laboratory, Argonne, Illinois 60439*

³*Istituto Nazionale di Fisica Nucleare, University of Bologna, I-40127 Bologna, Italy*

⁴*Brandeis University, Waltham, Massachusetts 02254*

⁵*University of California at Los Angeles, Los Angeles, California 90024*

⁶*Instituto de Fisica de Cantabria, CSIC-University of Cantabria, 39005 Santander, Spain*

⁷*Enrico Fermi Institute, University of Chicago, Chicago, Illinois 60637*

⁸*Joint Institute for Nuclear Research, RU-141980 Dubna, Russia*

⁹*Duke University, Durham, North Carolina 27708*

¹⁰*Fermi National Accelerator Laboratory, Batavia, Illinois 60510*

¹¹*University of Florida, Gainesville, Florida 32611*

¹²*Laboratori Nazionali di Frascati, Istituto Nazionale di Fisica Nucleare, I-00044 Frascati, Italy*

¹³*University of Geneva, CH-1211 Geneva 4, Switzerland*

¹⁴*Harvard University, Cambridge, Massachusetts 02138*

¹⁵*Hiroshima University, Higashi-Hiroshima 724, Japan*

¹⁶*University of Illinois, Urbana, Illinois 61801*

¹⁷*The Johns Hopkins University, Baltimore, Maryland 21218*

¹⁸*Institut für Experimentelle Kernphysik, Universität Karlsruhe, 76128 Karlsruhe, Germany*

¹⁹*Korean Hadron Collider Laboratory: Kyungpook National University, Taegu 702-701,*

Seoul National University, Seoul 151-742

and SungKyunKwan University, Suwon 440-746, Korea

²⁰*High Energy Accelerator Research Organization (KEK), Tsukuba, Ibaraki 305, Japan*

²¹*Ernest Orlando Lawrence Berkeley National Laboratory, Berkeley, California 94720*

²²*Massachusetts Institute of Technology, Cambridge, Massachusetts 02139*

²³*Institute of Particle Physics: McGill University, Montreal H3A 2T8*

and University of Toronto, Toronto, Canada M5S 1A7

²⁴*University of Michigan, Ann Arbor, Michigan 48109*

²⁵*Michigan State University, East Lansing, Michigan 48824*

²⁶*University of New Mexico, Albuquerque, New Mexico 87131*

²⁷*The Ohio State University, Columbus, Ohio 43210*

²⁸*Osaka City University, Osaka 588, Japan*

²⁹*University of Oxford, Oxford OX1 3RH, United Kingdom*

³⁰*Universita di Padova, Istituto Nazionale di Fisica Nucleare, Sezione di Padova, I-35131 Padova, Italy*

³¹*University of Pennsylvania, Philadelphia, Pennsylvania 19104*

³²*Istituto Nazionale di Fisica Nucleare, University and Scuola Normale Superiore of Pisa, I-56100 Pisa, Italy*

³³*University of Pittsburgh, Pittsburgh, Pennsylvania 15260*

³⁴*Purdue University, West Lafayette, Indiana 47907*

³⁵*University of Rochester, Rochester, New York 14627*

³⁶*Rockefeller University, New York, New York 10021*

³⁷*Rutgers University, Piscataway, New Jersey 08855*

³⁸*Texas A&M University, College Station, Texas 77843*

³⁹*Texas Tech University, Lubbock, Texas 79409*

⁴⁰*Istituto Nazionale di Fisica Nucleare, University of Trieste/Udine, Italy*

⁴¹*University of Tsukuba, Tsukuba, Ibaraki 305, Japan*

⁴²*Tufts University, Medford, Massachusetts 02155*

⁴³*Waseda University, Tokyo 169, Japan*

⁴⁴*University of Wisconsin, Madison, Wisconsin 53706*

⁴⁵*Yale University, New Haven, Connecticut 06520*

(Received 25 April 2000)

We have measured the polarization of J/ψ and $\psi(2S)$ mesons produced in $p\bar{p}$ collisions at $\sqrt{s} = 1.8$ TeV, using data collected at the Collider Detector at Fermilab during 1992–1995. The polarization of promptly produced J/ψ [$\psi(2S)$] mesons is isolated from those produced in B -hadron decay, and measured over the kinematic range $4 [5.5] < P_T < 20$ GeV/ c and $|y| < 0.6$. For $P_T \geq 12$ GeV/ c we do not observe significant polarization in the prompt component.

PACS numbers: 13.85.Qk, 13.20.Gd, 13.88.+e, 14.40.Gx

The production of heavy quarkonia states, $c\bar{c}$ and $b\bar{b}$, provides a useful system for the study of quantum chromodynamics (QCD), as it involves both perturbative and nonperturbative energy scales. In $p\bar{p}$ collisions, charmonium production occurs through three mechanisms: direct production, the decay of heavier charmonia, and the decay of b -flavored hadrons. The first two mechanisms are collectively known as “prompt” because they are observed to occur at the $p\bar{p}$ interaction point.

The Collider Detector at Fermilab (CDF) Collaboration previously reported results on the production of J/ψ and $\psi(2S)$ mesons [1,2]. The measured cross sections for direct production were on the order of 50 times larger than predicted by the color singlet model [3]. However, calculations based on the nonrelativistic QCD (NRQCD) factorization formalism [4,5] are able to account for the observed cross sections by including color octet production mechanisms. This leads to the prediction that directly produced ψ mesons will be increasingly transversely polarized at high P_T [5–7]. [In this Letter we use ψ to denote either J/ψ or $\psi(2S)$ mesons.] This is because the production of ψ mesons with $P_T \gg M_\psi$ is dominated by gluon fragmentation. It is predicted that the gluon’s transverse polarization is preserved as the $c\bar{c}$ pair evolves into a bound state ψ meson. On the other hand, the color evaporation model predicts an absence of polarization [8]. In this Letter, we report on measurements of the polarization of promptly produced ψ mesons at CDF. Our analysis also yields as a by-product the effective polarization of the ψ mesons produced in B -hadron decays.

CDF is a multipurpose detector designed to study high energy $p\bar{p}$ collisions produced by the Fermilab Tevatron [9]. The CDF coordinate system is defined with the z axis along the proton beam direction. The polar angle θ is defined relative to the z axis, r is the perpendicular radius from this axis, and ϕ is the azimuthal angle. Pseudorapidity is defined as $\eta \equiv -\ln[\tan(\theta/2)]$. Three charged-particle tracking detectors immersed in a 1.4 T solenoidal magnetic field surround the beam line. This tracking system is contained within a calorimeter, while drift chambers outside the calorimeter identify muon candidates.

The innermost tracking device is a 4-layer silicon microstrip detector (SVX) located at radii between 2.9 and 7.9 cm from the beam axis. The SVX is surrounded by a set of time projection chambers extending out to a radius of 22 cm. An 84-layer cylindrical drift chamber (CTC) measures the particle trajectories in the region between 30 and 132 cm from the beam. This tracking

system has high efficiency for detecting charged particles with momentum transverse to the beam $P_T > 0.4$ GeV/ c and $|\eta| \leq 1.1$. Together, the CTC and SVX measure charged-particle transverse momenta with a precision of $\sigma_{P_T}/P_T = 0.007 \oplus 0.001P_T$ (with P_T in GeV/ c). The impact parameter resolution is $\sigma_d = (13 + 40/P_T)$ μm for tracks with SVX and CTC information.

The central muon detection system consists of four layers of planar drift chambers separated from the interaction point by five interaction lengths of material. This system detects muons with $P_T \geq 1.4$ GeV/ c and $|\eta| \leq 0.6$. Dimuon candidates used in this analysis are collected using a 3-level $\mu^+\mu^-$ trigger. The first-level trigger requires that two candidates be observed in the muon chambers. For each muon candidate the first-level trigger efficiency rises from $\sim 40\%$ at $P_T = 1.5$ GeV/ c to $\sim 93\%$ for muons with $P_T > 3.0$ GeV/ c . The second-level trigger requires one or more charged particle tracks in the CTC, reconstructed using the central fast tracker (CFT). The CFT performs a partial reconstruction of all charged tracks with P_T above ~ 2 GeV/ c . Muon candidates found by the first-level trigger are required to match a CFT track within 15° in azimuth. The third-level trigger performs three-dimensional track reconstruction and accepts dimuon masses in a broad window around the J/ψ and $\psi(2S)$ masses.

The data used in this study correspond to an integrated luminosity of 110 pb^{-1} and were collected between 1992 and 1995. Following the online data collection, additional requirements are made offline to identify the signals and to reduce the backgrounds. To identify muon candidates and reduce the rate from sources such as π/K meson decay-in-flight, we require that each track observed in the muon chambers be associated with a matching CTC track. These matches are required to pass a maximum χ^2 cut of 9 and 12 (for 1 degree of freedom) in the ϕ and z views, respectively. Also, we require P_T greater than about 2 GeV/ c for each muon candidate. This requirement ensures that the muon trigger and reconstruction efficiencies are well understood, to avoid biases in the decay angular distributions of the charmonia states studied below.

The measurement of the polarization of ψ mesons is made by analyzing their decays to $\mu^+\mu^-$ in the helicity basis, in which the spin quantization axis lies along the ψ direction in the $p\bar{p}$ center-of-mass (laboratory) frame. We define θ^* as the angle between the μ^+ direction in the ψ rest frame and the ψ direction in the laboratory frame. The normalized angular distribution $I(\cos\theta^*)$ is given by

$$I(\cos\theta^*) = \frac{3}{2(\alpha + 3)}(1 + \alpha \cos^2\theta^*). \quad (1)$$

Unpolarized ψ mesons have $\alpha = 0$, whereas $\alpha = +1$ or -1 corresponds to fully transverse or longitudinal polarizations, respectively. Experimentally, the acceptance is severely reduced as $|\cos\theta^*|$ approaches 1, due to the P_T cuts on the muons. Our method for determining α is to fit the observed distributions of $\cos\theta^*$ to distributions derived from simulated $\psi \rightarrow \mu^+ \mu^-$ decays. The Monte Carlo simulation accounts for the geometric and kinematic acceptance of the detector as well as the reconstruction efficiency as a function of $\cos\theta^*$.

In order to extract the polarization parameter α for promptly produced ψ mesons, we separate the prompt component from the B -decay component using the proper decay length of each event. For ψ candidates with one or both muons reconstructed in the SVX (the SVX sample), we define a vector point from the $p\bar{p}$ collision point to the ψ decay vertex. The transverse decay length L_{xy} is then defined as the projection of this vector onto the ψ transverse momentum. The proper decay length ct is related to the transverse decay length by $ct = (M_\psi L_{xy}) / (F_{\text{corr}}^\psi P_T^\psi)$, where M_ψ is the ψ mass. Here F_{corr}^ψ is a correction factor obtained from Monte Carlo studies [10], which accounts for the fact that we are using the ψ P_T instead of the B hadron P_T . Prompt events have ct consistent with zero, whereas B decays have an exponential ct distribution; the detector resolution smears the ct distribution. We fit the ct distribution to obtain the relative fractions of prompt and B -decay production. Details of this fitting procedure are given in [10]. The measured fraction of J/ψ mesons which come from B -hadron decay increases from $(13.0 \pm 0.3)\%$ at $P_T^{J/\psi} = 4 \text{ GeV}/c$ to $(40 \pm 2)\%$ at $20 \text{ GeV}/c$. For $\psi(2S)$ mesons, an increase from $(21 \pm 2)\%$ to $(35 \pm 4)\%$ is seen in the range from 5.5 to $20 \text{ GeV}/c$.

The proper decay length measurement allows us to divide the data into two samples: a short-lived sample dominated by prompt production and a long-lived sample dominated by B decays. The short-lived sample is defined by $-0.1 \leq ct \leq 0.013[0.01] \text{ cm}$, and the long-lived sample by $0.013[0.01] \leq ct \leq 0.3 \text{ cm}$, for the J/ψ [$\psi(2S)$] analyses, respectively. The boundary between the two ct regions has been optimized separately for the J/ψ and $\psi(2S)$ samples, to maximize the purity of prompt decays in the short-lived sample and B decays in the long-lived sample. Depending on P_T^ψ , the prompt fraction in the short-lived sample ranges from 85% [86%] to 96% [95%], and the B -decay fraction in the long-lived sample ranges from 83% [86%] to 98% [91%], for J/ψ [$\psi(2S)$], respectively.

The J/ψ polarization is measured in seven P_T bins, covering a range of 4–20 GeV/c . Using a 3 standard deviation mass window around the J/ψ peak, our data sample consists of 180 000 signal J/ψ events, with a signal-to-background ratio of about 13. The J/ψ sample is divided

into three subsamples: the short-lived and long-lived SVX samples described above, and a third sample (the CTC sample) in which neither muon has SVX information and no ct measurement is made. In each $P_T^{J/\psi}$ bin, we measure the prompt polarization (α_P) and the effective polarization of J/ψ mesons from B -hadron decays (α_B). (We refer to α_B as “effective” because θ^* is defined by using the lab frame, not the B -hadron rest frame—in effect this dilutes any polarization from the B decay toward zero.) We find that it is not feasible to make separate polarization measurements for direct J/ψ production and for production from χ_c and $\psi(2S)$ decays. The latter sources account for $(36 \pm 6)\%$ of the prompt component, with only a small $P_T^{J/\psi}$ dependence [2].

The J/ψ polarization is measured by fitting $\cos\theta^*$ distributions in data to a set of Monte Carlo templates [11]. The templates are generated by processing simulated samples of $J/\psi \rightarrow \mu^+ \mu^-$ decays with a detector and trigger simulation. The polarization is obtained using a χ^2 fit of the data to a weighted sum of transversely polarized and longitudinally polarized templates. The fitted weights yield the polarization. Two transverse/longitudinal template pairs are generated, using measured prompt and B -decay $P_T^{J/\psi}$ spectra [1]. The $\cos\theta^*$ distribution of background events is modeled in the fit using sidebands around the J/ψ mass peak. The fit is performed simultaneously on the SVX short-lived, SVX long-lived, and CTC samples, with two fit parameters: α_P and α_B . To account for the mixture of prompt and B -decay components in each sample, the relative fractions of prompt and B -decay templates in each are fixed in the fit using the results of the lifetime fit. The B -decay fraction in the CTC sample is assumed to be the

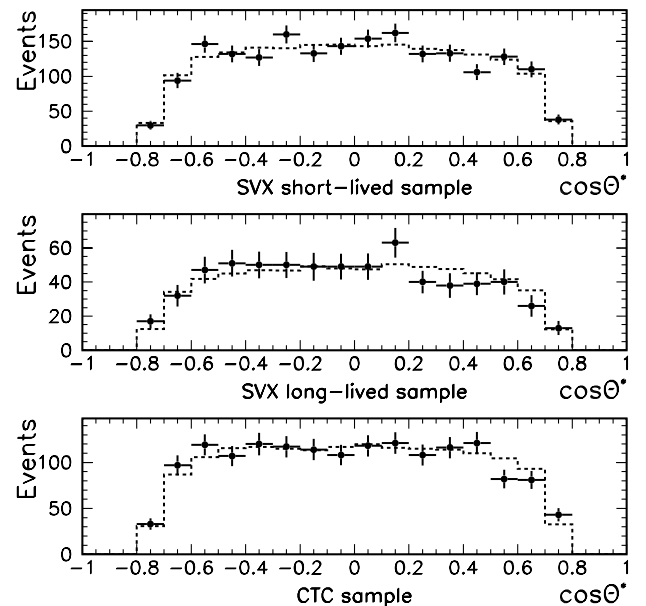


FIG. 1. The J/ψ polarization fit to $\cos\theta^*$ distributions in the 12–15 GeV/c bin. Points: sideband-subtracted data in the SVX short-lived, SVX long-lived, and CTC samples. Dashed lines: fit.

TABLE I. Fit results for J/ψ polarization, with statistical and systematic uncertainties.

P_T bin (GeV/c)	Mean P_T (GeV/c)	α_P	α_B
4–5	4.5	$0.30 \pm 0.12 \pm 0.12$	$-0.49 \pm 0.41 \pm 0.13$
5–6	5.5	$0.01 \pm 0.10 \pm 0.07$	$-0.18 \pm 0.33 \pm 0.07$
6–8	6.9	$0.178 \pm 0.072 \pm 0.036$	$0.10 \pm 0.20 \pm 0.04$
8–10	8.8	$0.323 \pm 0.094 \pm 0.019$	$-0.06 \pm 0.20 \pm 0.02$
10–12	10.8	$0.26 \pm 0.14 \pm 0.02$	$-0.19 \pm 0.23 \pm 0.02$
12–15	13.2	$0.11 \pm 0.17 \pm 0.01$	$0.11 \pm^{0.31}_{0.28} \pm 0.02$
15–20	16.7	$-0.29 \pm 0.23 \pm 0.03$	$-0.16 \pm^{0.38}_{0.33} \pm 0.05$

same as in the SVX sample, because the two samples differ primarily in the z position of the primary vertex. Within each $P_T^{J/\psi}$ bin, a small correction is applied to the $P_T^{J/\psi}$ distributions of the Monte Carlo samples so that they match with those in the data. As an example, the fit in the P_T range, 12–15 GeV/c, is shown in Fig. 1.

Three sources of systematic uncertainty are evaluated: the trigger efficiency, the fitted prompt and B -decay fractions, and the $P_T^{J/\psi}$ spectra used in making the Monte Carlo templates. Except in the lowest P_T bins, the systematic uncertainties are much smaller than the statistical uncertainties. Our fit results are listed in Table I, and α_P is compared with a theoretical NRQCD prediction [7] in Fig. 2.

The measurement of the $\psi(2S)$ polarization is made in three P_T bins covering 5.5–20.0 GeV/c. Both muons are

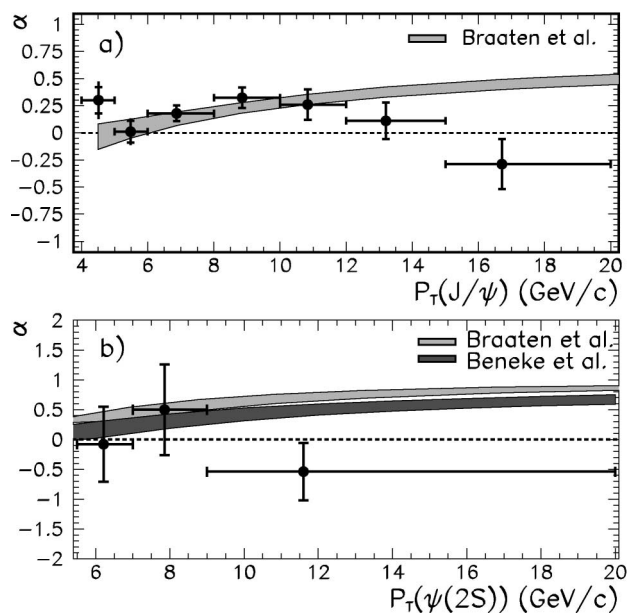


FIG. 2. (a) The fitted polarization of prompt J/ψ mesons for $|y^{J/\psi}| < 0.6$. Full error bars denote statistical and systematic uncertainties added in quadrature; ticks denote statistical errors alone. The shaded band shows a NRQCD factorization prediction [7] which includes the contribution from χ_c and $\psi(2S)$ decays. (b) The fitted polarization of prompt $\psi(2S)$ mesons for $|y^{\psi(2S)}| < 0.6$. Error bars denote statistical and systematic uncertainties added in quadrature. Shaded bands show two NRQCD factorization predictions [6,7].

required to be reconstructed in the SVX. The resulting dimuon mass distribution is fitted with a Gaussian signal and a linear background. We find a total of 1855 ± 65 signal $\psi(2S)$ events, with a signal-to-background ratio of about 1 in a 3 standard deviation mass window around the $\psi(2S)$ mass.

As discussed above, the sample in each P_T bin is further divided into two subsamples based on the ct distribution. Because the statistics are lower than in the J/ψ case, we use ten bins in $|\cos\theta^*|$. The number of signal events in each $|\cos\theta^*|$ bin is obtained by fitting its mass distribution. The resulting $|\cos\theta^*|$ distributions in the two ct subsamples are fitted simultaneously to the predicted number of events to extract the $\psi(2S)$ polarizations for prompt and B -decay production. The number of predicted events in each $|\cos\theta^*|$ bin is derived by weighting the normalized angular distribution $I(\cos\theta^*)$ with the detector acceptance [12]. We use the measured prompt and B -decay $P_T^{\psi(2S)}$ distributions [1] to calculate the acceptance. As in the J/ψ case, there is a small correlation between the measured $P_T^{\psi(2S)}$ distributions and the polarization. A correction is

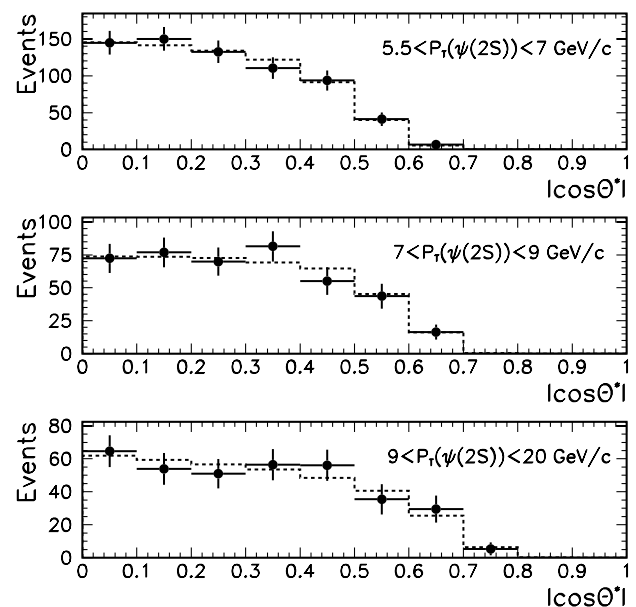


FIG. 3. Fits to $|\cos\theta^*|$ distributions in the short-lived $\psi(2S)$ data sample, in the three P_T bins. Points: data. Dashed lines: fit. The acceptance extends farther out in $|\cos\theta^*|$ as P_T increases.

TABLE II. Fit results for $\psi(2S)$ polarization, with statistical and systematic uncertainties.

P_T bin (GeV/c)	Mean P_T (GeV/c)	α_P	α_B
5.5–7.0	6.2	$-0.08 \pm 0.63 \pm 0.02$	$-0.26 \pm 1.26 \pm 0.04$
7.0–9.0	7.9	$0.50 \pm 0.76 \pm 0.04$	$-1.68 \pm 0.55 \pm 0.12$
9.0–20.0	11.6	$-0.54 \pm 0.48 \pm 0.04$	$0.27 \pm 0.81 \pm 0.06$

applied iteratively in the fits to account for this dependence. Figure 3 shows the observed angular distributions with their polarization fits for the short-lived sample in the three $P_T^{\psi(2S)}$ bins.

Three sources of systematic uncertainty are considered: the uncertainty in the event yield from the mass fits in the $|\cos\theta^*|$ bins, the uncertainty due to the error on the fitted prompt and B -decay fractions, and the uncertainty on the $|\cos\theta^*|$ acceptance from the Monte Carlo modeling of the $P_T^{\psi(2S)}$ distributions. The uncertainty due to the trigger efficiency is negligible in the $P_T^{\psi(2S)}$ range used. The systematic uncertainties are much smaller than the statistical uncertainties. The fitted values of α_P and α_B as a function of $P_T^{\psi(2S)}$ are listed in Table II, and α_P is shown in Fig. 2 with the NRQCD predictions [6,7].

In conclusion, we have measured the polarization of J/ψ and $\psi(2S)$ mesons produced in 1.8 TeV $p\bar{p}$ collisions. The polarization from B decays is generally consistent with zero, as expected. In both the J/ψ and $\psi(2S)$ cases, we do not observe increasing prompt transverse polarization at $P_T \gtrsim 12$ GeV/c. Our measurements are limited by statistics, especially for the $\psi(2S)$, but they appear to indicate that no large transverse prompt polarization is present at high P_T , in disagreement with NRQCD factorization predictions.

We thank the Fermilab staff and the technical staffs of the participating institutions for their vital contributions. This work was supported by the U.S. Department of Energy and National Science Foundation, the Italian Istituto Nazionale di Fisica Nucleare, the Ministry of Education, Science, Sports and Culture of Japan, the Natural Sciences and Engineering Research Council of Canada, the Na-

tional Science Council of the Republic of China, the Swiss National Science Foundation, the A. P. Sloan Foundation, and the Bundesministerium für Bildung und Forschung, Germany.

-
- [1] The CDF Collaboration, F. Abe *et al.*, Phys. Rev. Lett. **79**, 572 (1997).
 - [2] The CDF Collaboration, F. Abe *et al.*, Phys. Rev. Lett. **79**, 578 (1997).
 - [3] M. Cacciari and M. Greco, Phys. Rev. Lett. **73**, 1586 (1994); E. Braaten *et al.*, Phys. Lett. B **333**, 548 (1994); D. P. Roy and K. Sridhar, Phys. Lett. B **339**, 141 (1994).
 - [4] G. Bodwin, E. Braaten, and G. Lepage, Phys. Rev. D **51**, 1125 (1995); **55**, 5853(E) (1997); E. Braaten and S. Fleming, Phys. Rev. Lett. **74**, 3327 (1995); M. Cacciari *et al.*, Phys. Lett. B **356**, 553 (1995); E. Braaten and Y. Chen, Phys. Rev. D **54**, 3216 (1996); P. Cho and A. K. Leibovich, Phys. Rev. D **53**, 150 (1996); *ibid.* **53**, 6203 (1996).
 - [5] P. Cho and M. Wise, Phys. Lett. B **346**, 129 (1995).
 - [6] M. Beneke and M. Krämer, Phys. Rev. D **55**, 5269 (1997).
 - [7] E. Braaten, B. Kniehl, and J. Lee, hep-ph/9911436.
 - [8] J. Amundson *et al.*, Phys. Lett. B **390**, 323 (1997).
 - [9] The CDF Collaboration, F. Abe *et al.*, Nucl. Instrum. Methods Phys. Res., Sect. A **271**, 387 (1998); The CDF Collaboration, F. Abe *et al.*, Phys. Rev. D **52**, 4784 (1995); P. Azzi *et al.*, Nucl. Instrum. Methods Phys. Res., Sect. A **360**, 137 (1995).
 - [10] The CDF Collaboration, F. Abe *et al.*, Phys. Rev. D **57**, 5382 (1998).
 - [11] R. Cropp, Ph.D. thesis, University of Toronto, 2000.
 - [12] C.-Y. P. Ngan, Ph.D. thesis, Massachusetts Institute of Technology, 2000.